

Electronic Structure, Methyl Group Reorientation and Reactions of Radical Cations of 1,2,4-Trimethylcyclohexanes: An EPR Study

Masaru Shiotani,^{*,a} Michinobu Matsumoto^a and Mikael Lindgren^b

^a Department of Applied Chemistry, Faculty of Engineering, Hiroshima University, 0724 Higashi-Hiroshima, Japan

^b Department of Physics and Measurement Technology, Linköping University of Technology, S-581 83 Linköping, Sweden

Two isomeric radical cations of 1,2,4-Me₃-cyclohexane, *r*-1,*t*-2,*t*-4-Me₃-c-C6⁺ and *r*-1,*t*-2,*c*-4-Me₃-c-C6⁺, have been studied at cryogenic temperatures adopting the halocarbon matrix technique. Both isomer cations show the same EPR hyperfine (hf) pattern with a triplet of triplets with $a_1^H = 60$ G (2 H) and $a_2^H = 32$ G (2 H) at 4.2 K. The hf parameters coincide with those of the *cis* and *trans* isomers of the 1,2-Me₂-c-C6 cation, implying a similar electronic ground state structure in which the main part of the unpaired electron resides in the C-1–C-2-σ-bond. The EPR spectra show a reversible temperature change between *ca.* 77 and 180 K. The temperature-dependent spectra can be explained by a dynamic effect in which the methyl groups on C-1 and C-2 rotate. Adopting a three-site jump model the rate constants were evaluated to be *ca.* 5.0×10^6 s⁻¹ (100 K) to *ca.* 5.0×10^7 s⁻¹ (180 K) with an activation energy of 1.1 kcal mol⁻¹. This low activation energy is compared to methyl rotation in radical cations of propane⁺ and butane⁺, and is discussed in terms of the unpaired electron distribution within the framework of carbon atoms. Furthermore, it is shown that secondary and tertiary alkyl radicals are predominantly formed by thermal reactions of *r*-1,*t*-2,*t*-4-Me₃-c-C6⁺ and *r*-1,*t*-2,*c*-4-Me₃-c-C6⁺, respectively, in the CF₃-c-C₆F₁₁ matrix.

The study of radical cations of saturated hydrocarbons by EPR spectroscopy was introduced with the halocarbon matrix isolation technique at the end of the 1970s.¹⁻² Cyclic alkanes with degenerate HOMOs (Highest Occupied Molecular Orbitals) have attracted attention due to the possibility of having Jahn–Teller distorted ground states.³ A degenerate HOMO can also be split by introducing substituents, which has encouraged us to investigate a variety of alkyl-substituted cyclohexane cations.⁴ It has also been established that cations of cyclic alkanes can exist with different ground states; recent studies of the *cis* and *trans* decalin cations⁵ and certain isomers of 1,3-dimethyl-, 1,3,5-trimethyl- and 1,2,3-trimethyl-cyclohexane^{4a,h} cations revealed the coexistence of two different ground states in several cases with the relative populations determined by the matrix and temperature.

This report concerns the radical cations of two isomers of 1,2,4-trimethylcyclohexane; 1,*trans*-2,*trans*-4-trimethylcyclohexane (*r*-1,*t*-2,*t*-4-Me₃-c-C6⁺) and 1,*trans*-2,*cis*-4-trimethylcyclohexane (*r*-1,*t*-2,*c*-4-Me₃-c-C6⁺). It is shown that at low temperature (4.2 K) the cationic structure is distorted (C₁) with one elongated C-1–C-2 bond in which a large fraction of the unpaired electron resides. A similar distorted electronic structure has been observed in our recent studies on the radical cations of methylcyclohexane,^{4a-d} 1,1-dimethylcyclohexane,^{4d} 1,2-dimethylcyclohexane^{4c} and methylsilacyclohexane.⁶ The reversible temperature effect on the EPR line shape between *ca.* 77 and 180 K was studied using c-C₆F₁₂ and CF₂BrCF₂Br as matrices, and could be explained by assuming a three-site jump model to take account of methyl group reorientation. The activation energy of the process is evaluated to be 1.1 kcal mol⁻¹. The value is compared with those reported for related systems. Furthermore, it is found that secondary and tertiary alkyl radicals are predominantly formed by thermal reaction of *r*-1,*t*-2,*t*-4-Me₃-c-C6⁺ and *r*-1,*t*-2,*c*-4-Me₃-c-C6⁺, respectively, in the CF₃-c-C₆F₁₁ matrix.

The geometric structures and numbering of atoms of the two *cis*- and *trans*-isomers of 1,2-dimethyl- and 1,2,4-trimethyl-

cyclohexane discussed in this study are shown overleaf; a chair conformation has been assumed for the cyclohexane ring.

Experimental

The solutes and matrices were obtained commercially (Fluka and/or Tokyo Kagaku Seiki Co.) and used without further purification. The solutes were mixed with the matrix (1 mol% unless otherwise specified) on a vacuum line using standard techniques. The radical cations were generated at 77 or 4.2 K by γ-ray irradiation. This is a well established method to generate and stabilize the solute radical cation.¹⁻⁴ The EPR spectra were recorded using a Bruker ESP 300E spectrometer from 4 K to the temperature at which all radicals decayed.

The EPR spectra simulations of the three-site jump model were carried out employing a program for calculating exchange-broadened isotropic spectra developed by Heinzer.⁸ The program is based on the equation of motion of the density matrix within the Liouville formalism. The software was implemented and run on a HITAC M-680H computer.

The geometry optimizations were carried out by employing the semi-empirical MNDO MO method, the program MOPAC/386, based on the MOPAC 5.0 (QCPE No. 455), of TORAY system centre, and the *ab initio* MO method (Gaussian 90/STO-3G) on a Convex/C3240 computer at Information Processing Centre, Hiroshima University. The spin density and ¹H hyperfine (hf) splittings were calculated using the INDO MO method⁸ for the optimized geometries. The same approach has previously proved successful in the prediction of the spin density distribution of a large number of related cation radicals.⁴

Results

Low Temperature Spectra and Electronic Ground States.—The experimental EPR spectrum shown in Fig. 1 (upper) was measured for the *r*-1,*t*-2,*t*-4-Me₃-c-C6 cation radical formed by

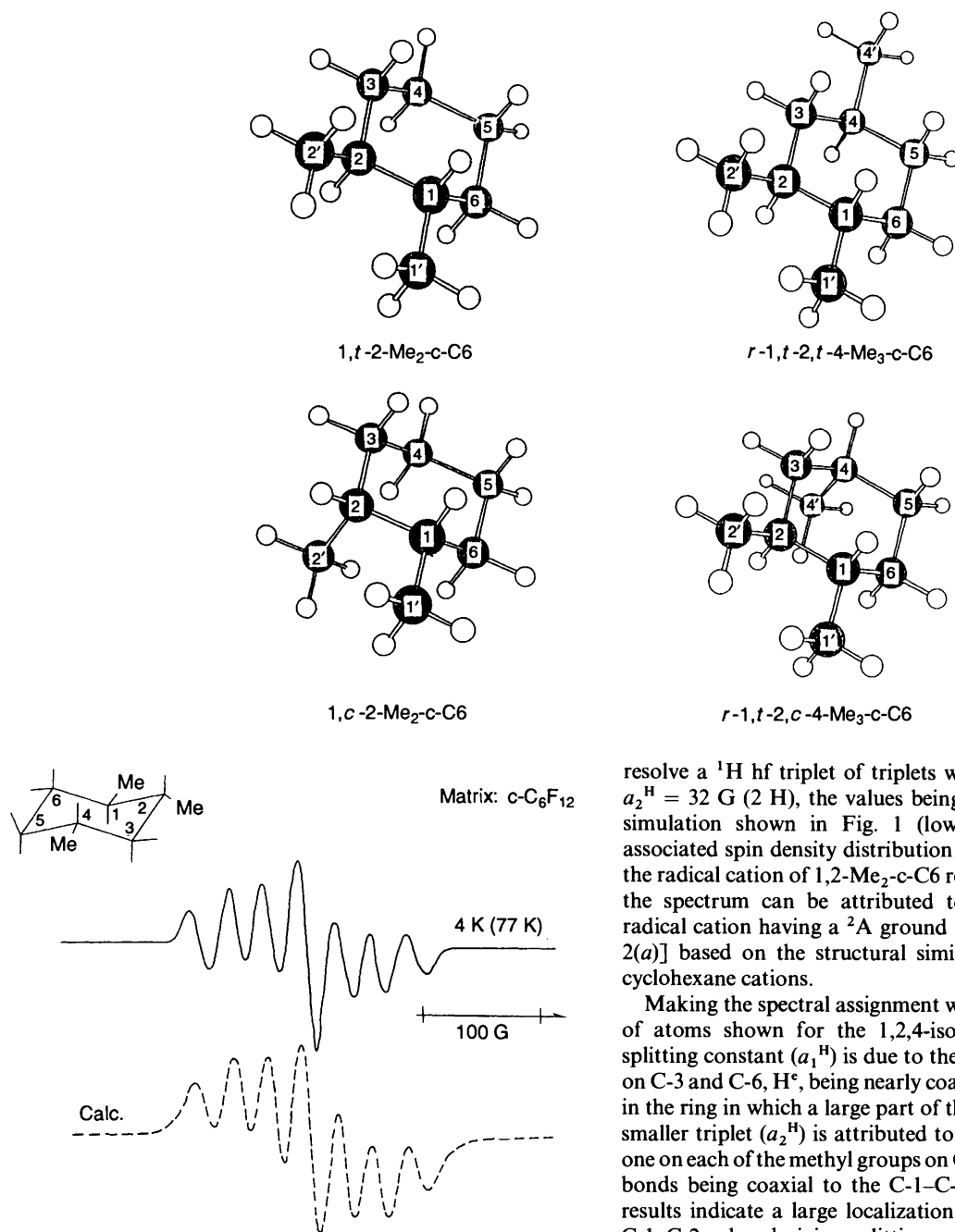


Fig. 1 The EPR spectrum of $r-1,t-2,t-4-Me_3-c-C_6^+$ observed at 4.2 K (upper). The radical cation was generated by γ -irradiation of 1 mol% of $r-1,t-2,t-4-Me_3-c-C_6^+$ in $c-C_6F_{12}$ at 77 K. The spectral line shape was essentially the same in the temperature range 4.2–77 K. The dotted lines (lower) show the spectrum simulated using the 1H hf splittings of $a_1^H = 60$ G (2 H) and $a_2^H = 32$ G (2 H).

ionizing irradiation at 77 K in the $c-C_6F_{12}$ matrix. The same spectrum was obtained using the $CF_3-c-C_6F_{11}$ and CF_2Br-CF_2Br matrices. An essentially identical spectrum was also observed for the $r-1,t-2,c-4-Me_3-c-C_6^+$ isomer (not shown). No apparent change in spectral line-shape could be detected in the temperature range between 77 and 4.2 K. Furthermore, no spectral difference was observed for samples irradiated and measured at 4.2 K. Above *ca.* 100 K the spectrum changed reversibly with temperature. This could be explained by adopting a dynamic three-site jump model for the reorientation of methyl hydrogens attached to C-1 and C-2 and will be discussed in a following section.

All the low temperature EPR spectra (4.2–77 K) clearly

resolve a 1H hf triplet of triplets with $a_1^H = 60$ G (2 H) and $a_2^H = 32$ G (2 H), the values being derived from the spectral simulation shown in Fig. 1 (lower). The hf features and associated spin density distribution are almost coincident with the radical cation of 1,2- Me_2-c-C_6 reported previously.^{4c} Thus, the spectrum can be attributed to the $r-1,t-2,t-4-Me_3-c-C_6$ radical cation having a 2A ground state in C_1 symmetry [Fig. 2(a)] based on the structural similarity to the 1,2-dimethylcyclohexane cations.

Making the spectral assignment with reference to numbering of atoms shown for the 1,2,4-isomers above, the large hf splitting constant (a_1^H) is due to the equatorial ring hydrogens on C-3 and C-6, H^e , being nearly coaxial with the C-1–C-2 bond in the ring in which a large part of the spin density resides. The smaller triplet (a_2^H) is attributed to two methyl hydrogens H^m , one on each of the methyl groups on C-1' and C-2', with the C–H bonds being coaxial to the C-1–C-2 bond. The experimental results indicate a large localization of the spin density to the C-1–C-2 σ -bond giving splittings of *ca.* 30 G due to the pair of methyl hydrogens through a hyperconjugative mechanism. No 1H splitting ascribable to the 'third' methyl group on C-4 was detected. These findings are in agreement with earlier conclusions. Further details of electronic structure and spin delocalization mechanisms in substituted cyclohexane cation radicals are given in previous reports.⁴

The structure of $r-1,t-2,t-4-Me_3-c-C_6^+$ was examined by adopting the semi-empirical MNDO MO calculations searching for energy minima along three different molecular distortions: (a) C-1–C-2 bond elongation, (b) simultaneous C-2–C-3 and C-3–C-4 bond elongations, and (c) C-2–C-3 bond elongation. The optimized bond lengths are summarized in Figs. 2(b) and 3 together with the 1H hf values calculated by using the INDO method of the optimized geometries. The calculated results of (a) reproduce well the experimental hf splittings. Also the heat of formation of this structure is the lowest. Although the spin densities on the methyl hydrogens at C-1 and C-2 are overestimated by *ca.* 10% compared to the experiments it can be concluded that spin density is attracted mainly to the C-1–C-2 σ -bond giving large and resolvable

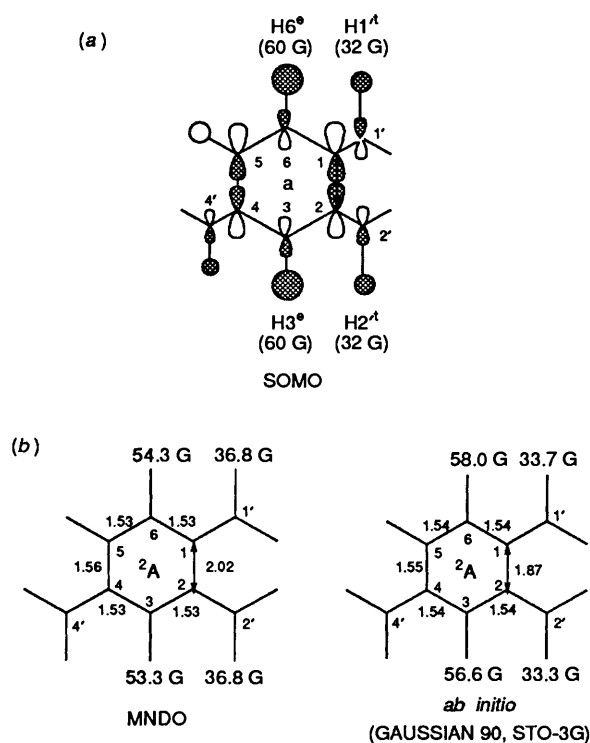


Fig. 2 (a) The a SOMO in C_1 proposed for $r-1,t-2,t-4\text{-Me}_3\text{-c-C}_6^+$ together with the assignment of experimental ^1H hf splittings of $a_1^{\text{H}} = 60\text{ G}$ (2 H) and $a_2^{\text{H}} = 32\text{ G}$ (2 H). (b) The C-C bond lengths (in Å) of the optimized geometry of $r-1,t-2,t-4\text{-Me}_3\text{-c-C}_6^+$ calculated by the semi-empirical (MNDO, left) and *ab initio* (GAUSSIAN, right) MO methods together with the isotropic ^1H hf splittings (in G) estimated by the INDO method for the optimized geometries.

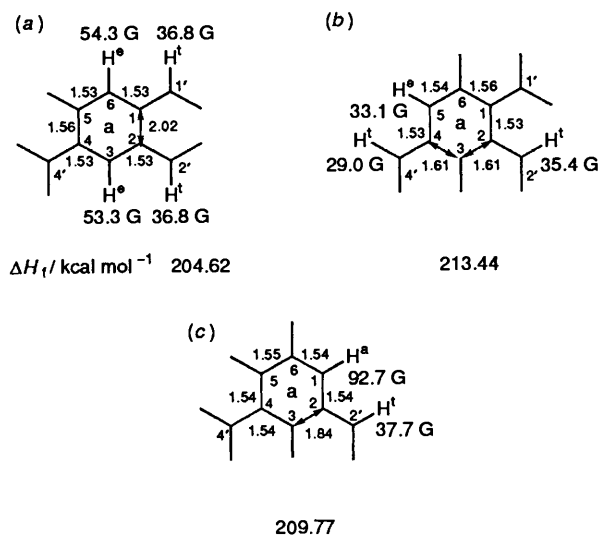


Fig. 3 Calculated isotropic ^1H hf splittings (in G) for the equatorial hydrogens in the optimized geometry (MNDO) of $r-1,t-2,t-4\text{-Me}_3\text{-c-C}_6^+$ in three possible cases: (a) C-1-C-2 bond elongation; (b) simultaneous C-2-C-3 and C-3-C-4 bond elongation; (c) C-2-C-3 bond elongation. The calculated heats of formation ΔH_f (kcal mol^{-1}) are also given.

splittings due to the pair of methyl hydrogens. As a consequence, no hf splitting ascribable to the 'third' methyl hydrogen can be detected.

In agreement with the MNDO results the *ab initio* MO calculations support the SOMO (singly occupied molecular orbital) of a in C_1 proposed for $r-1,t-2,t-4\text{-Me}_3\text{-c-C}_6^+$. The agreement between the experimental and calculated ^1H hf splittings is slightly improved as seen in Fig. 2(b) (right). It

should also be mentioned that the C-1-C-2 bond is predicted about 10% shorter in the *ab initio* calculation. Thus, the MNDO overestimates the geometrical distortion since the *ab initio* results can be considered more accurate. Furthermore, the *ab initio* results predict an almost undistorted structure for the remaining parts of the molecule. The molecular distortion therefore seems very localized to the σ -bond containing the unpaired electron.

Temperature-Dependent EPR Spectra and Line-Shape Simulations.—The reversible EPR line-shapes of $r-1,t-2,t-4\text{-Me}_3\text{-c-C}_6^+$ in two different matrices, $\text{c-C}_6\text{F}_{12}$ and $\text{CF}_2\text{BrCF}_2\text{Br}$, recorded in the temperature range between 4.2 and 200 K, are shown in Figs. 4 (left) and 5 (left), respectively. The line shape differs slightly using these two matrices. It has been observed that no appreciable changes in the spectra were observed between 4.2 and 77 K in both matrices. Above *ca.* 100 K the spectrum starts to change from the original seven lines into a triplet of *ca.* 60 G (2 H) with partially resolved septet of *ca.* 11 G (6 H) at the high temperature limit. The reversible line-shape can be explained adopting a three-site jump model depicted in Fig. 6 (top). In this model the six hydrogens of two methyl groups on C-1 and C-2 jump by 120° at the same time with rate constant, k (s^{-1}), the life time of each conformation being $1/k$ (s): the correlated three-site jump model.

The reorientation of the methyl groups does not affect the large splitting (a_1^{H}) due to the two equatorial ring protons on C-3 and C-6, which, together with the smaller methyl splitting (a_2^{H} ; each on C-1' and C-2'), make up the dominating features of the EPR line shape at the rigid limit (4–77 K). This supports our previous assignment of the ^1H hf splittings in $1,2\text{-Me}_2\text{-c-C}_6^+$.^{4c} Above *ca.* 77 K the methyl group rotation starts to affect the overall EPR line-shape. This is explained by introducing pairwise magnetically equivalent methyl groups in which one hydrogen with the splitting a_2^{H} (32 G) is exchanging with the two other methyl hydrogens, the splittings of the latter were treated as parameters. The best fit values, $a_3^{\text{H}} = 9\text{ G}$ and $a_4^{\text{H}} = 3\text{ G}$, were found by examining a series of combinations in simulating the temperature dependent line shapes. Fig. 6 (stick plots) illustrates how the line broadening and line-shifts are caused by the methyl group rotation in the system of the two magnetically equivalent methyl groups with one large (a_2^{H}) and two small (a_3^{H} , a_4^{H}) sets of hf splitting. Thus, at the rapid exchange limit the EPR line shape changes to a convolution of the rigid 1:2:1 triplet of the ring hydrogens with the binomially distributed septet due to six equivalent methyl hydrogens.

By introducing the correlated three site jump model the experimental line shapes at different exchange rates were examined. The best-fit simulated spectra are shown in Figs. 4 (right) and 5 (right) with the exchange rate constants k (s^{-1}) inserted: the rates lay between *ca.* $5 \times 10^6\text{ s}^{-1}$ (100 K) and *ca.* $5 \times 10^7\text{ s}^{-1}$ (180 K). The radical cations of $r-1,t-2,c-4\text{-Me}_3\text{-c-C}_6$ and $1,t-2\text{-Me}_2\text{-c-C}_6$ were found to give similar temperature-dependent EPR spectra (not shown here).

The Arrhenius plots of the rates, k (s^{-1}) vs. $1/T$ (K^{-1}) for the different cases of matrices and cation isomers are given in Fig. 7. The rates for various temperatures follow a straight line. From the slope the energy of activation was evaluated to be 1.1 kcal mol^{-1} . The activation energies for methyl group rotation in related systems are collected in Table 1.

Reactions.—Upon annealing the sample above a phase transition of the matrix used, the radical cations were irreversibly changed into neutral radicals by an apparent deprotonation reaction. It is found that the site of the alkyl radical formed is highly selective, in other words, only one major neutral radical product is formed among several possibilities. This site preference was found to be governed by

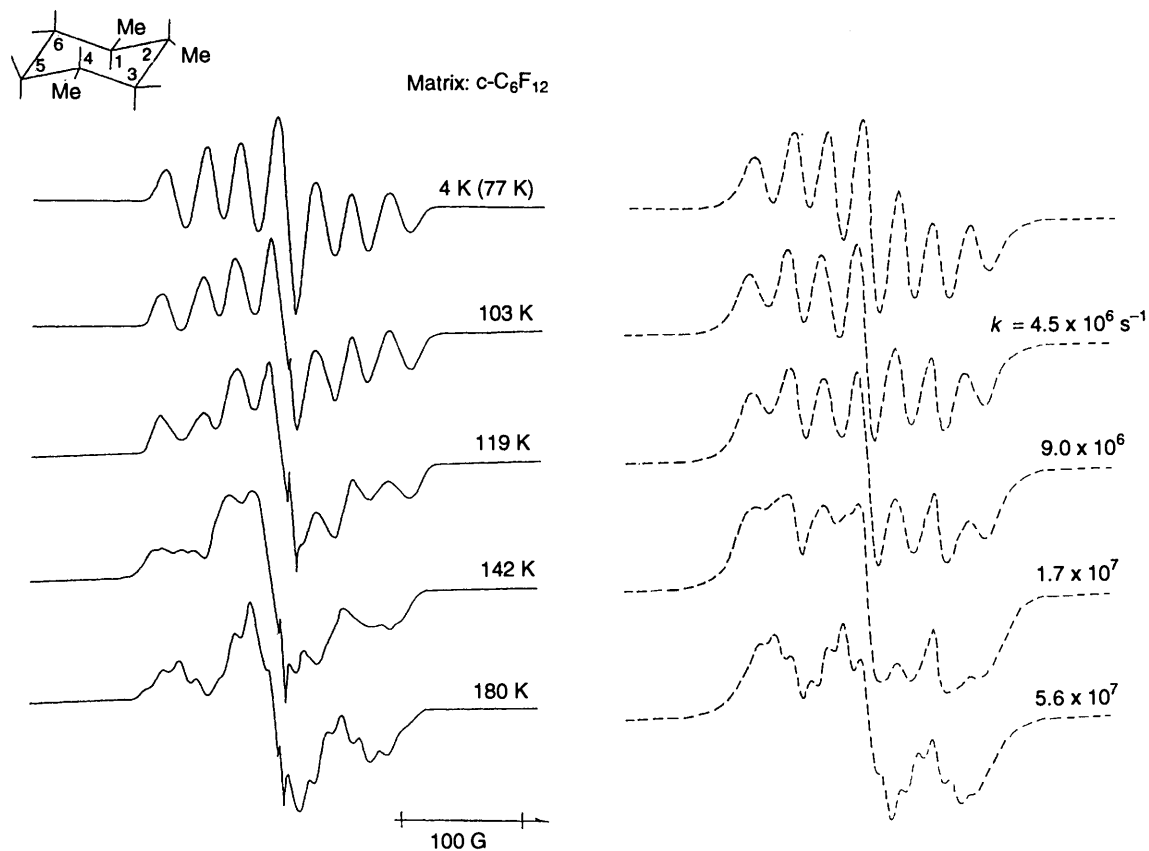


Fig. 4 The temperature dependent EPR spectra of $r\text{-}1,t\text{-}2,t\text{-}4\text{-Me}_3\text{-}c\text{-C}_6^+$ in $c\text{-C}_6\text{F}_{12}$ in the temperature range between 77 and 180 K (left). Simulations of the 'double' methyl group rotation at different rates adopting the model discussed in the text (right). The ^1H hf splittings used: $a_1^{\text{H}} = 60 \text{ G}$ (2 H) (ring hydrogens not exchanging), $a_2^{\text{H}} = 32 \text{ G}$ (2 H), $a_3^{\text{H}} = 9 \text{ G}$ (2 H) and $a_4^{\text{H}} = 3 \text{ G}$ (2 H). For assignment see schemes in the text. Rates are inserted.

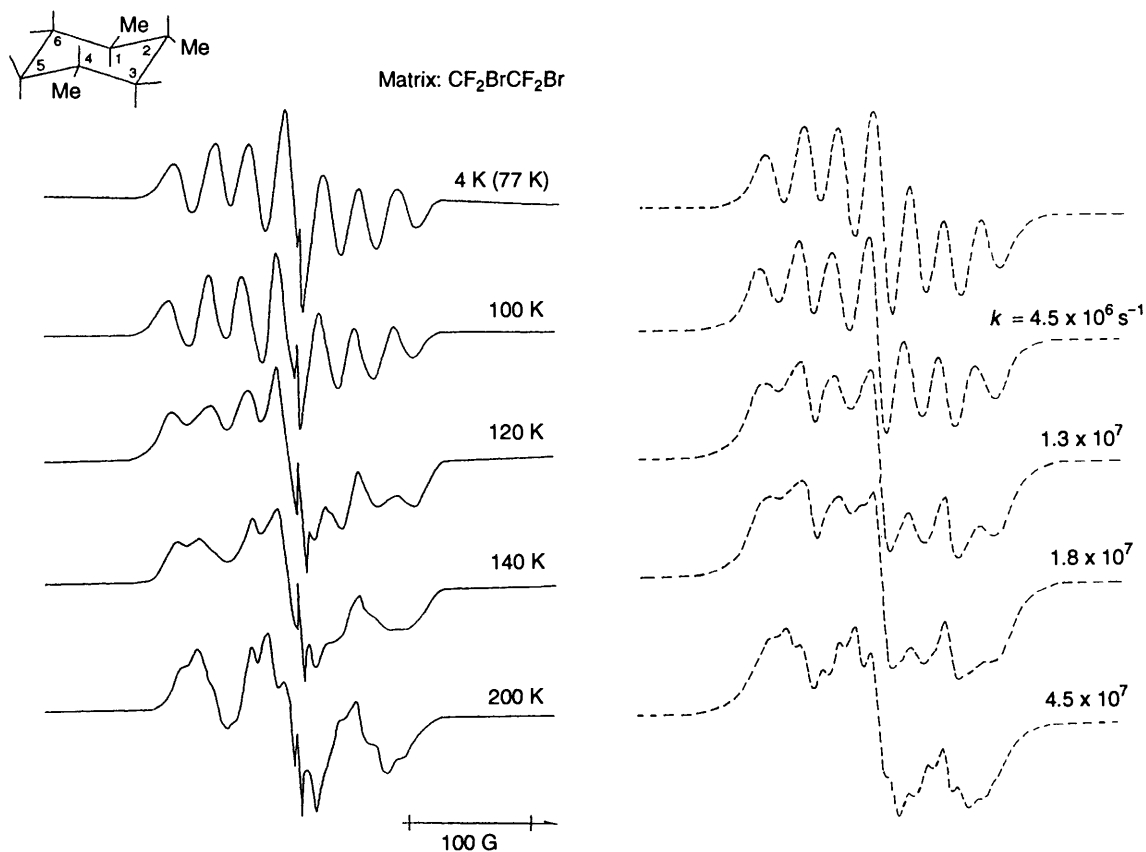


Fig. 5 The temperature dependent EPR spectra of $r\text{-}1,t\text{-}2,t\text{-}4\text{-Me}_3\text{-}c\text{-C}_6^+$ in $\text{CF}_2\text{BrCF}_2\text{Br}$ in the temperature range between 77 and 200 K (left). The line shape simulations are with the same model and hf parameters as in Fig. 4 (right).

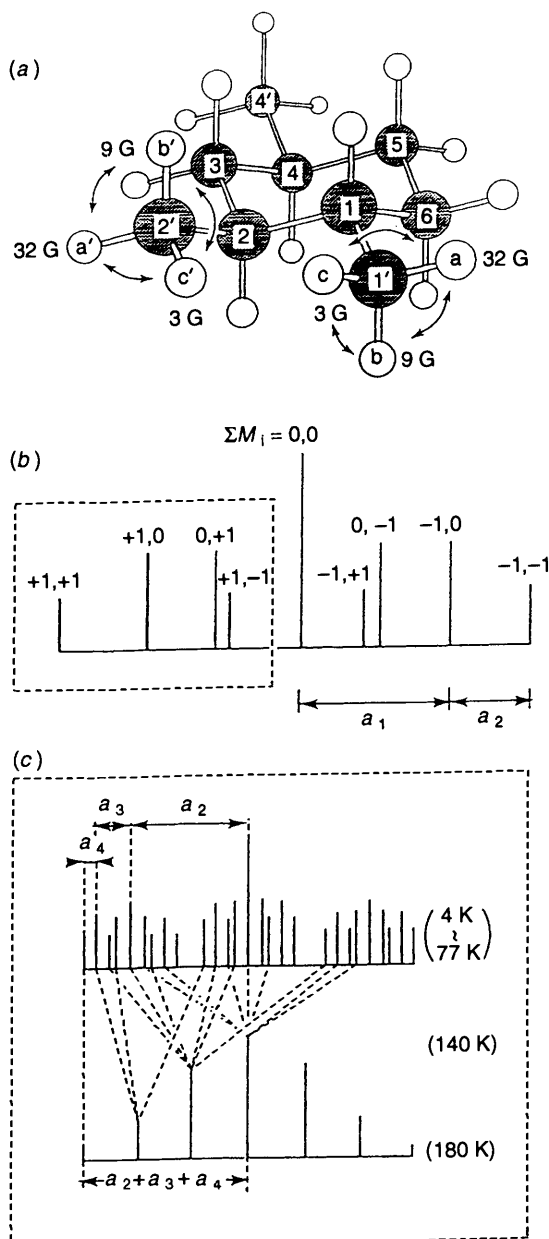


Fig. 6 (a) The 'correlated' three site jump model of methyl group rotation used for the simulation of the temperature-dependent EPR line shapes. (b) Stick plot of the dominating ^1H hf pattern of the rigid-limit EPR spectrum observed at 4.2 K (77 K). (c) Illustration showing how the EPR line positions are altered with increasing temperature: the temperature accelerates the methyl group rotation.

the detailed position of the methyl groups on the ring structure, *i.e.*, *cis* or *trans*. As an example we can consider the spectrum shown in Fig. 8(a). The spectrum of the radical cation of *r-1,t-2,t-4-Me₃-c-C6⁺* disappears as the temperature is increased up to *ca.* 190 K, under which a spectrum of a neutral radical evolves. Details of the analysis are given in the captions of Fig. 8. The secondary alkyl radical [Fig. 9(c)] is contributing more than 80% of the total intensity. The radical cation of *r-1,t-2,c-4-Me₃-c-C6⁺* follows a similar decay, however, the radical species formed takes a completely different EPR spectrum. The analysis (caption to Fig. 8) shows that a tertiary alkyl radical has been formed in more than 90% of the total intensity. The possible locations of alkyl radicals in the ring structure are shown in Fig. 7. As can be seen, there are three cases for each of the secondary and tertiary positions. From the spectrum analysis the radical formed from *r-1,t-2,t-4-Me₃-c-C6⁺* must

Table 1 Summary of experimental activation energy reported for methyl group rotation in some ionic systems related to this study

Ion/Molecule	Matrix/Phase	$E_a/\text{kcal mol}^{-1}$	Ref.
C_2H_6	gas	2.9	11
C_3H_8^+	SF_6	2.5	12
$\text{C}_4\text{H}_{10}^+$	CFCl_3	2.3	12
$1,2,4\text{-Me}_3\text{-c-C6}^+$	$\text{c-C}_6\text{F}_{12}$	1.1	this work
CH_3COOH^-	crystal	2.2	9, 10

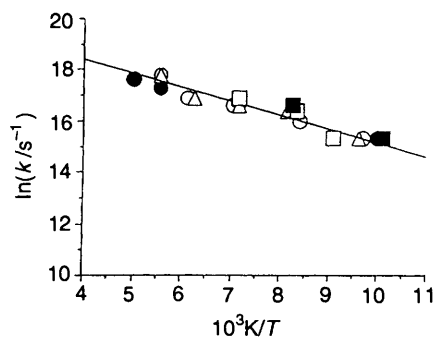
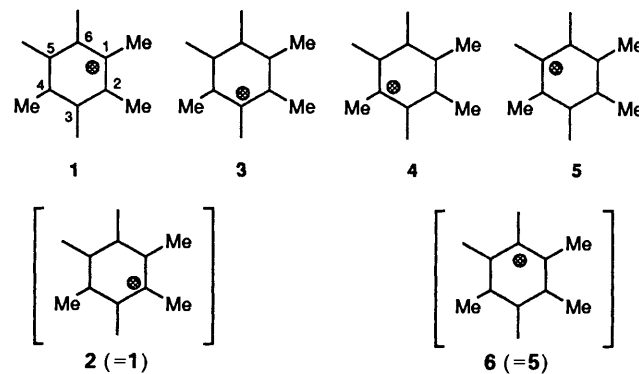


Fig. 7 The Arrhenius plot of the rate, k (s^{-1}) vs. $10^3\text{K}/T$ of isomer radical cations of 1,2- $\text{Me}_2\text{-c-C6}$ and 1,2,4- $\text{Me}_3\text{-c-C6}$ in the two different matrices indicated. \square : 1^+ , 1, *t-2-Me₂-c-C6⁺*/ $\text{CF}_2\text{BrCF}_2\text{Br}$. \blacksquare : 2^+ , 1, *c-2-Me₂-c-C6⁺*/ $\text{CF}_2\text{BrCF}_2\text{Br}$. \circ : 3^+ , *r-1,t-2,t-4-Me₃-c-C6⁺*/ $\text{c-C}_6\text{F}_{12}$. \bullet : 3^+ , $\text{c-C}_6\text{F}_{12}$. Δ : 4^+ , *r-1,t-2,c-4-Me₃-c-C6⁺*/ $\text{c-C}_6\text{F}_{12}$. The straight line corresponds to an activation energy of 1.1 kcal mol^{-1} .



originate from case 3 since only this position gives two large hf splittings due to β -hydrogens. From a similar analysis of the *r-1,t-2,c-4-Me₃-c-C6⁺* case it can be concluded that structure 4 is dominating. In conclusion, there is a selective route in the formation of alkyl radicals from the parent cation radical in these matrix. This is in agreement with our earlier finding for 1,2-dimethyl-substituted cyclohexanes.^{4f} Thus, the appearance of an axial methyl group gives predominantly a tertiary radical, whereas in the cases where only equatorial methyl groups can be considered, a secondary alkyl radical is formed. Thus, in the *trans* isomer (*r-1,t-2,t-4-*) the deprotonation occurs at a hydrogen with high spin density whereas in the *cis* isomer (*r-1,t-2,c-4-*) a hydrogen with negligible spin density is deprotonated. This contradicts the idea argued by Toriyama *et al.*¹³ as well as recent results of Stienlet and Ceulemans,¹⁴ that is, the deprotonation occurs in the cation radical at a hydrogen with high spin density.

Discussion

Structure.—This study presents the experimental data of two isomer radical cations of 1,2,4-trimethylcyclohexanes. Previously we have elucidated the electronic structures of a variety of alkyl-substituted cyclohexane cations, in particular, of the cases with alkyl groups in two positions, such as *cis*- and *trans*-

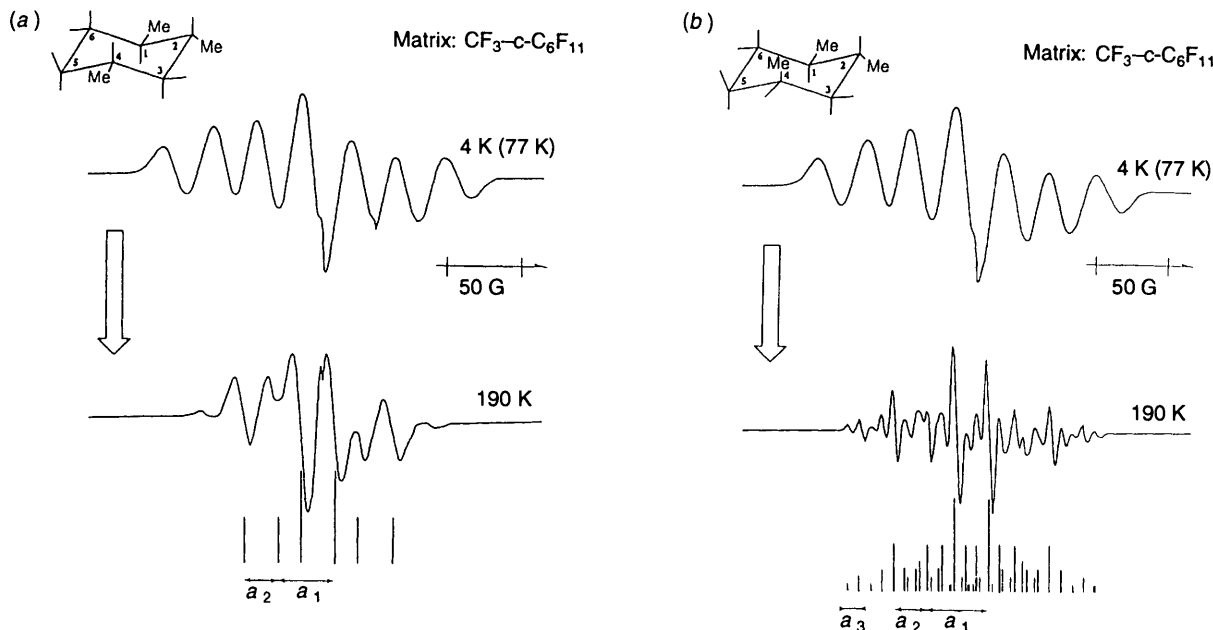


Fig. 8 The EPR spectra of (a) *r*-1,*t*-2,*t*-4- Me_3 -*c*- C_6^+ and (b) *r*-1,*t*-2,*c*-4- Me_3 -*c*- C_6^+ are irreversibly changed into those of alkyl radicals upon annealing the samples to *ca.* 190 K in the CF_3 -*c*- C_6F_{11} matrix. The stick plots correspond to: (a) $a_1 = 38$ G (2 H) and $a_2 = 23$ G (2 H); (b) $a_1 = 41$ G (2 H), $a_2 = 23$ G (3 H) and $a_3 = 8$ G (2 H). For assignment of the alkyl radical formed see Fig. 9.

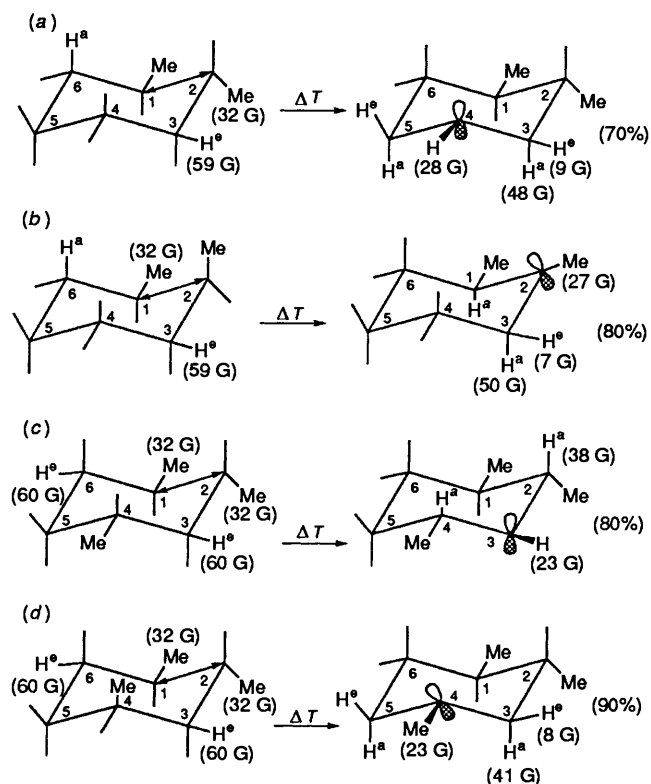


Fig. 9 Assignment of the alkyl radicals (right) formed during the decay of the corresponding radical cations (left). The number (%) is the relative yield of the depicted alkyl radical. The experimental ^1H hf splittings are given at appropriate positions. The arrows indicate a prolonged C-C bond.

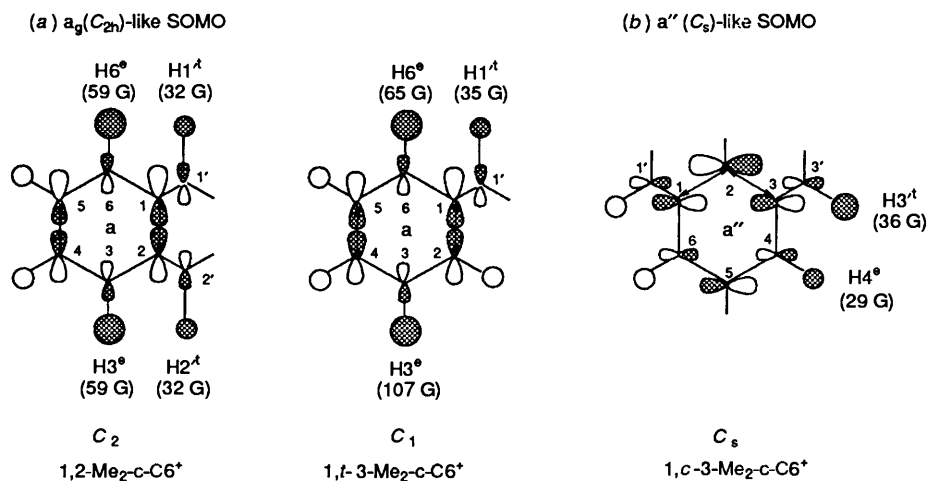
isomers of 1,1-, 1,2-, 1,3- and 1,4-dimethylcyclohexane.⁴ It was found that the SOMOs of the methyl group substituted cyclohexane cations can be classified into three orbitals which resemble a_g , b_g or a'' , following a Jahn-Teller distortion of the e_g HOMO of cyclohexane.^{4c} The selection of SOMO depends on isomer and matrix. For example, the *trans*-isomer cation of 1,3- Me_2 -*c*- C_6 with one axial methyl group has been found to take an a_g -like SOMO (more exactly a in C_1), in a variety of

matrices used, with a large hf splitting of 107 G for the equatorial hydrogen attached to the axially substituted ring carbon.^{4c,g} Whereas, the *cis*-isomer cation of 1,3- Me_2 -*c*- C_6 shows contributions from both a_g -like and b_g -like SOMOs in the $\text{CF}_2\text{ClCFCl}_2$ matrix, but exclusively from a b_g -like SOMO (a'' in C_2) in the *c*- C_6F_{12} matrix.^{4g} On the other hand both isomer cations of 1,2- Me_2 -*c*- C_6 take a_g -like SOMOs [a in C_1 (*cis*) and a in C_2 (*trans*)], in the matrices used, with a hf splitting of 59 G in the equatorial hydrogens located coaxially to the C-1-C-2 bond as discussed above.

The isomer cations of 1,2,4- Me_3 -*c*- C_6 presented in this study were found to have a SOMO with resemblance to the isomers of 1,2- Me_2 -*c*- C_6^+ since almost identical EPR spectra were obtained in both systems at low temperature. This result suggests that the SOMO of 1,2,4- Me_3 -*c*- C_6^+ is controlled by two methyl groups attached to the adjacent C-1 and C-2 positions, but not on C-2 and C-4, the latter corresponding to the structure of 1,3- Me_2 -*c*- C_6^+ . The addition of one methyl group to 1,2- Me_2 -*c*- C_6^+ makes, however, the cation more stable, so as to permit observation of the EPR spectra at higher temperatures than for 1,2- Me_2 -*c*- C_6^+ in the same matrix. The reason is not clear now, but it might be related to the trapping site of the radical cation, for example, interstitial, or to the substitutional position.

The structure of the cyclohexane cations having three methyl groups are similar to the 1,2-substituted cases as discussed in the experimental section. The calculation we present here (*ab initio*) gives further support to our earlier suggestions that the unpaired electron is localised mainly on one C-C bond, and that the unpaired spin density is transferred by a hyperconjugation mechanism to two equatorial hydrogens and two methyl hydrogens of which the corresponding C-H bonds are all nearly coaxial with the C-C bond containing the unpaired electron.

Dynamics.—From the correlated three-site exchange model the temperature-dependent EPR spectra of 1,2- Me_2 -*c*- C_6^+ and 1,2,3- Me_3 -*c*- C_6^+ were analysed qualitatively, and an activation energy of *ca.* 1.1 kcal mol⁻¹ was evaluated for the process. In Table 1 the activation energies of related methyl group rotations are collected. As noted, the barrier for methyl group rotation of 1,2,4- Me_3 -*c*- C_6^+ is considerably lower than that

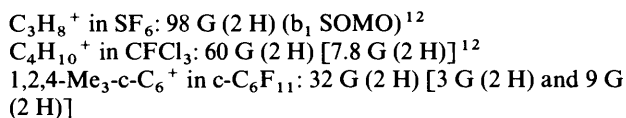


found for both the propane and the butane cations, and the neutral ethane molecule, see Table 1. (A comparison with the ethane cation is not relevant since the dynamic process is described by a different physical process, a pseudo rotation.¹⁵)

The internal rotation of the methyl group in acetic acid has been examined extensively (refs. 9, 10 and refs. therein). In this case the internal barrier of methyl rotation has been interpreted as a measure of non-planarity around the radical centre.¹¹ Thus neutral acetic acid gives a low barrier (ca. 0.5 kcal mol⁻¹) compared to that of the anion (2.2 kcal mol⁻¹) which is known to have a bent radical centre.^{9,10}

Applying similar arguments for 1,2,4-Me₃-c-C6⁺, the small internal methyl group rotation barrier could be due to a more pronounced sp² character for the methine carbons (C-1 and C-2) at which most of the spin density is localized, compared with the C-2 carbon in propane⁺, the C-2 and C-3 fragments in butane⁺ or -CH₃ fragments of ethane, which would have more sp³ character. In a review of calculated methyl-rotation barriers in ethane the actual value was attributed to the degree of overlap repulsion of the orbitals constituting the C-1-H and C-2-H bonds.¹¹

An alternative mechanism for the lower activation energy may be related to degree of hyperconjugation, that is, the transfer of unpaired electron density to the *trans* hydrogens of the methyl groups on C-1 and C-2. The large barrier would here be related to the hyperfine splittings of the methyl hydrogens attached to the C-C bond containing the larger fraction of spin density. Some relevant cases are listed below.



In view of the few studies of methyl group rotation of alkane cations in freons reported so far we regard the explanation of the low barrier for methyl group rotation in 1,2,4-Me₃-c-C6⁺ as tentative. Particularly, the role of the matrix (external forces) in the methyl group rotation barriers needs to be studied more systematically.

Comments on the Dynamic Simulations.—As found by inspecting Figs. 4 and 5 the EPR line shapes are reasonably reproduced towards the low and high temperature limits. At intermediate temperatures the agreement is less satisfactory. This is probably due to the approximation of making a simple 'correlated' three-site model from a physically more stringent random-jump nine-site model.

Since the spectra near the high and low temperature limits are

reproduced fairly well it is assumed that the energy of activation would not be much different using a more sophisticated model; the detailed nature of the exchange in this case might be revealed. It should also be noted in this context that Toriyama *et al.* employed the same qualitative approach (correlated three-site exchange) in the study of 'double methyl group rotation' in propane⁺ and butane⁺,¹² and obtained reasonable activation energies compared with data of neutral molecules.

The work to refine the modelling of double-methyl rotation by allowing exchange of six hydrogens in nine sites has been initiated.¹⁶

Acknowledgements

The authors thank Dr. Nikolas P. Benetis for helpful discussion on the dynamics of the methyl group reorientation. The present research was partially supported by the Subsidy for Scientific Research of the Ministry of Education in Japan (Grant No. 0464073) and the Swedish Natural Science Research Council (NFR).

References

- 1 A. Lund and M. Shiotani eds., *Radical Ionic Systems*, Kluwer, Dordrecht 1991.
- 2 For reviews, see (a) T. Shida, E. Haselbach and T. Bally, *Acc. Chem. Res.*, 1984, **17**, 180; (b) M. C. R. Symons, *Chem. Soc. Rev.*, 1984, 393; (c) M. Shiotani, *Magn. Reson. Rev.*, 1987, **12**, 333.
- 3 (a) M. B. Huang, S. Lunell and A. Lund, *Chem. Phys. Lett.*, 1983, **99**, 201; (b) S. Lunell, M. B. Huang, O. Claesson and A. Lund, *J. Chem. Phys.*, 1985, **82**, 5121; (c) K. Ohta, H. Nakatsuji, H. Kubodera and T. Shida, *Chem. Phys.*, 1983, **76**, 271; (d) M. Iwasaki, K. Toriyama and K. Nunome, *J. Chem. Soc., Chem. Commun.*, 1983, 202; (e) K. Toriyama, K. Nunome and M. Iwasaki, *J. Chem. Soc., Chem. Commun.*, 1984, 143; (f) S. Lunell, M. B. Huang and A. Lund, *Faraday Discuss. Chem. Soc.*, 1984, **78**, 35.
- 4 (a) M. Shiotani, N. Ohta and T. Ichikawa, *Chem. Phys. Lett.*, 1988, **149**, 185; (b) M. Lindgren, M. Shiotani, N. Ohta, T. Ichikawa and L. Sjöqvist, *Chem. Phys. Lett.*, 1989, **161**, 127; (c) M. Shiotani, M. Lindgren and T. Ichikawa, *J. Am. Chem. Soc.*, 1990, **112**, 967; (d) M. Shiotani, M. Lindgren, N. Ohta and T. Ichikawa, *J. Chem. Soc., Perkin Trans. 2*, 1991, 771; (e) L. Sjöqvist, M. Lindgren and M. Shiotani, *J. Chem. Soc., Faraday. Trans.*, 1990, **86**, 3377; (f) M. Shiotani, M. Lindgren, F. Takahashi and T. Ichikawa, *Chem. Phys. Lett.*, 1990, **170**, 201; (g) M. Lindgren, M. Matsumoto and M. Shiotani, *J. Chem. Soc., Perkin Trans. 2*, 1992, 1397; (h) M. Lindgren, N. P. Benetis, M. Matsumoto and M. Shiotani, manuscript in preparation.
- 5 (a) V. I. Melekov, O. A. Anisimov, L. Sjöqvist and A. Lund, *Chem. Phys. Lett.*, 1990, **174**, 95; (b) M. V. Barnabas and A. D. Trifunac, *Chem. Phys. Lett.*, 1991, **187**, 565.
- 6 M. Shiotani, K. Komaguchi, J. Ohshita and M. Ishikawa, *Chem. Phys. Lett.*, 1992, **188**, 93.
- 7 J. Heinzer, *Mol. Phys.*, 1971, **22**, 167; *QCPE (Quantum Chemistry Program Exchange) Program No. 207*, Indiana University, 1972.

- 8 *QCPE* No. 506. The same approach has been used to investigate a number of related cations, see refs. 4 (c), (d), (g).
- 9 R. Erickson, U. Nord, N. P. Benetis and A. Lund, *Chem. Phys.*, 1992, **168**, 91.
- 10 D. Suryanarangana and M. D. Sevilla, *J. Phys. Chem.*, 1980, **84**, 3045.
- 11 R. M. Pitzer, *Acc. Chem. Res.*, 1983, **16**, 207, 15.
- 12 (a) K. Matsuura, K. Nunome, K. Toriyama and M. Iwasaki, *J. Phys. Chem.*, 1989, **93**, 149; (b) M. Iwasaki and K. Toriyama, *J. Am. Chem. Soc.*, 1986, **108**, 6441.
- 13 (a) K. Toriyama, K. Nunome and M. Iwasaki, *J. Chem. Phys.*, 1982, **77**, 5891; (b) K. Toriyama, K. Nunome and M. Iwasaki, *J. Phys. Chem.*, 1986, **90**, 6836.
- 14 D. Steinlet and J. Ceulemans, *J. Phys. Chem.*, 1992, **96**, 8751.
- 15 M. Iwasaki, K. Toriyama and K. Nunome, *Chem. Phys. Lett.*, 1984, **111**, 309.
- 16 Simulation programs based on Liouville formalism and chemical exchange in the Kaplan–Alexander limit is currently under development by Benetis and co-workers. (a) N. P. Benetis, D. J. Schneider and J. H. Freed, *J. Magn. Reson.*, 1989, **85**, 275; (b) N. P. Benetis, M. Lindgren, H.-S. Lee and A. Lund, *Appl. Magn. Reson.*, 1990, **1**, 267; (c) N. P. Benetis, L. Sjöqvist, A. Lund and J. Maruani, *J. Magn. Reson.*, 1991, **95**, 523; (d) L. Sjöqvist, N. P. Benetis, A. Lund and J. Maruani, *Chem. Phys.*, 1991, **156**, 457.

Paper 3/01998E

Received 30th March 1993

Accepted 12th May 1993